

# An Active Resonant Conductance Method for Design of Large Traveling-Wave-Fed SIW Linear Slot Arrays

Tongfei Yu<sup>\*</sup>, Zhengpeng Wang, Haibo Zhao, and Jungang Miao

**Abstract**—This paper presents an active resonant conductance method (ARCM) for the design of large traveling-wave-fed SIW linear slot arrays. Two key slot parameters, slot offsets and lengths, are derived from excitation coefficients with intermediary active resonant conductance. In this method, both dominant mode mutual coupling which includes external & internal and higher order modes mutual coupling are considered. An efficient way to derive active resonant conductance of slots in large slot arrays is proposed, which makes ARCM feasible for the design of large traveling-wave-fed linear slot arrays with high performance, e.g., low sidelobe level (SLL). Finally, a 16-slot and a 32-slot traveling-wave-fed SIW slot array antennas are designed. The processing of the 32-slot array design shows the efficiency of the proposed method for large arrays. The 16-slot array is fabricated and measured. Results from simulation and measurement verify the proposed method.

## 1. INTRODUCTION

Slot array antennas are preferred in many applications due to their high aperture efficiency, low sidelobe level, low cross polarization, and the ability of controlling the radiation patterns [1]. Traditionally, slot array antennas are constructed on metallic waveguides. Wu et al. [2–5] develop SIW based slot array antennas. SIW slot array antennas have the characteristics of small size, light weight, low profile, low cost and easy integration with other planar circuits, which attract many researchers.

In the previous study, almost all the SIW slot array antennas are designed by Elliott's method which considers mutual coupling among all the slots [5–11]. In Elliott's method [12–15], the required computation effort for the calculation of mutual coupling becomes enormous as the number of slots in the array increases. The iteration procedure to derive the physical parameters of slots also makes the design of a large SIW slot array complicated, and convergence problem may be encountered for large slot arrays [7]. Therefore, Elliott's method becomes unattractive for large array application [1].

The method in [1] can be applied to large arrays constructed on conventional waveguides. Based on power allocation technique, the iteration procedure is avoided, and the slot conductance can be directly derived from slot excitation. However, this method does not consider mutual coupling among slots. For SIW slot arrays, mutual coupling among slots becomes significant, even mutual coupling of high-order TE<sub>20</sub> mode cannot be ignored due to the reduced height, which makes this method unsuitable for the design of large SIW slot arrays.

The infinite array model for the design of large slot arrays is presented in [16]. Slot active admittance in the array environment is calculated by using the uniformly excited infinite array models. It is equal to the average slot active admittance of the arrays which approach a constant value as the array size increases. However, this method is mainly used for planar arrays, and the accuracy will decrease for linear arrays.

---

*Received 31 October 2016, Accepted 24 December 2016, Scheduled 9 January 2017*

<sup>\*</sup> Corresponding author: Tongfei Yu (ytfbuaa@ee.buaa.edu.cn).

The authors are with the School of Electronic and Information Engineering, Beihang University, 37th Xueyuan Road, Haidian District, Beijing 100191, China.

In this paper, an active resonant conductance method (ARCM) is proposed for the design of large traveling-wave-fed SIW linear slot arrays. Instead of computing mutual coupling among all the slots, active resonant conductance is calculated as intermediary step to synthesize the physical parameters of slots. In Section 2.1, active resonant conductance distribution of slots in the linear array is directly calculated from slot excitation coefficients based on power allocation technique. In Section 2.2, the relationships between active resonant conductance and physical parameters of slots including slot offsets and slot lengths are derived efficiently by uniformly excited finite array models. Then physical parameters of all the slots are determined using the above relationships. With the proposed method, a 16-slot and a 32-slot traveling-wave-fed SIW slot arrays are designed and simulated, respectively. The 16-slot array is fabricated and measured. Both simulation and measurement results are presented and discussed to verify the proposed method.

## 2. DESIGN PROCEDURE

At the beginning of the array design, the SIW geometry is designed following the rules in [3, 4] to satisfy center frequency requirement. Then using the equivalent formula for SIW [17], the design of an SIW slot array can be replaced with the design of a slot array on equivalent dielectric-filled rectangular waveguide to save huge simulation time and computation resources [5].

### 2.1. Active Resonant Conductance Distribution of Slot Array

A model of a traveling-wave-fed SIW linear longitudinal slot array is shown in Fig. 1. The longitudinal slots are alternatively displaced off the centerline of the SIW. It can be assumed that the radiated power of individual slot is proportional to the slot active conductance, and all the slots in the array are actively resonant at center frequency. The radiating slots can be modeled as shunt active resonant conductance, in this way, coupling from other slots is included. The equivalent circuit of the SIW slot array is shown in Fig. 2. Using the power allocation technique [1], active resonant conductance distribution of slots can be determined by the excitation coefficient of individual slot.

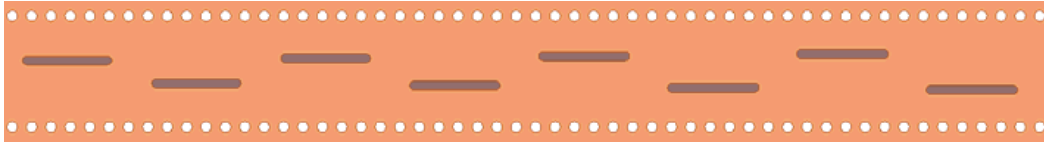


**Figure 1.** A model of Traveling-wave-fed SIW linear longitudinal slot array.

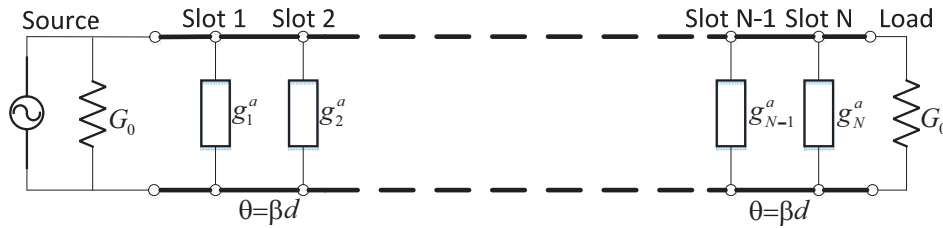


**Figure 2.** Equivalent circuit of the large traveling-wave-fed slot array.

The active resonant conductance  $g_i^a$  of the slot  $i$  is derived by power allocation at each slot:

$$g_1^a = \frac{P_1}{P_{in}} \quad (1)$$

$$g_i^a = \frac{P_i}{P_{in} - \sum_{j=1}^{i-1} P_j} \quad i = 2, 3, \dots, N \quad (2)$$

where  $P_{in}$  is the input power at the feeding port,  $P_i$  the power radiated by slot  $i$ .  $P_i = K A_i$ ,  $A_i$  is the excitation coefficient of slot  $i$ ,  $K$  the proportional factor and given by

$$K = \frac{P_{in} - P_l}{\sum_{i=1}^N A_i} \quad (3)$$

where  $P_l$  is the power absorbed by the matching load. It is pointed out that slot 1 is the slot closest to the feeding end of the SIW.

## 2.2. Active Resonant Conductance of Slots

The physical parameters of slots from the calculated active resonant conductance depend on the relationships of active resonant conductance and slot parameters. In a large slot array, the difference of mutual coupling between a central slot and a peripheral slot can be ignored, which is necessary to design a large SIW slot array. Thus, uniformly excited finite array model can be used to approximate the slot active resonant conductance in array environment. A large slot linear array consisting of slots with same offsets and lengths is constructed on the equivalent rectangular waveguide. The active admittance of all the slots in the constructed array are considered as the same value regardless of their positions. Changing the slot length in the constructed array, in this case, when maximum power is radiated and the minimum power are absorbed by the load, all the slots are actively resonant. Then active resonant conductance for the given slot offset can be calculated by the following formula:

$$g^a = 1 - \left( \frac{|S_{21}|^2}{1 - |S_{11}|^2} \right)^{\frac{1}{N}} \quad (4)$$

$N$  is the number of slots in the constructed array.  $S_{21}$  and  $S_{11}$  are simulated scattering parameters of the active resonant array. The corresponding slot length is defined as active resonant length. Thus, the active resonant length for the given slot offset is also obtained.

Repeating the above process for different slot offsets, the active resonant conductance and active resonant length as a function of slot offset can be derived by fitting the obtained data. With these two functions, slot offsets and lengths in the designed slot array can be directly derived from the active resonant conductance which have been calculated in Section 2.1.

## 2.3. Further Discussion

In theory, the finite array model to calculate active resonant conductance of slots in array environment has the same number of slots as that of the designed array. Then the computing effort will become enormous for a large array. However, according to our research, it is not necessary to consider all the slots for a large array. As a matter of fact, a constructed array with only a few slots is enough to derive the active resonant conductance accurately. The blue line with circles in Fig. 3 shows the active resonant conductance calculated with different numbers of slots finite array models. The orange line with squares shows the relative differences of the active resonant conductance. It can be seen that the derived active resonant conductance approaches a constant when the number of slots in the finite array model is more than 8. Therefore, the active resonant conductance can be derived with 8 slots finite array model only with minor difference. It makes the proposed method suitable for the design of a large traveling-wave-fed linear slot array.

## 3. SIMULATIONS

For verification purpose, a 16-slot and a 32-slot traveling-wave-fed SIW slot linear arrays with  $-25$  dB and  $-30$  dB Taylor distribution are designed by the proposed method. These arrays are designed on the substrate of Rogers RO4003C with dielectric constant of 3.55 and operate at 25.25 GHz. The thickness of the substrate is 1.524 mm, and that of the metal cladding is 0.017 mm. The width of SIW (vias center to vias center) is 5.1 mm corresponding to the width of 4.75 mm for the equivalent rectangular

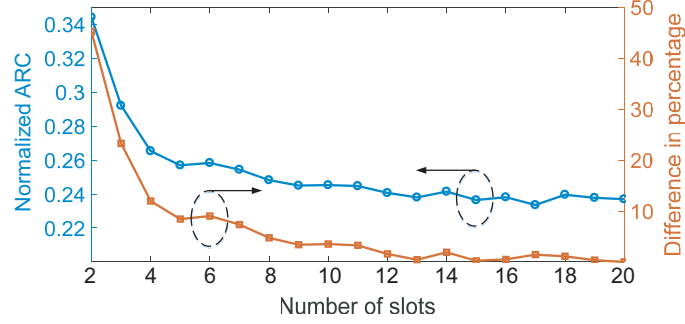


**Figure 3.** Normalized active resonant conductance (ARC) of slots versus number of slots in finite array model.

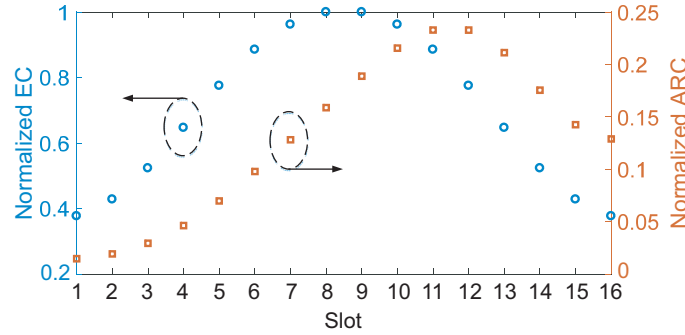


**Figure 4.** Normalized excitation coefficients (EC) and normalized active resonant conductance (ARC) of slots in the array.

waveguide. The spacing and diameter of the metalized vias are 0.9 mm and 0.5 mm, respectively. The slot width is 0.15 mm, and the slot is filleted with fillet radius 0.075 mm. The spacing of the slots is 6 mm so that the main beam points at an angle of  $\theta = 65.2$  degrees.

As traveling-wave-fed arrays, they must be terminated with a matching load to prevent reflecting wave. In order to stabilize the excitation of the last few slots before termination, about 5 to 10 percent of the power is passed and absorbed by the matching load. In our case, the power absorbed by the matching load is  $P_l/P_{in} = 0.05$ . Excitation coefficients of 16 slots for  $-25$  dB Taylor distribution are displayed in Fig. 4. By applying the proposed method, active resonant conductance distribution for the 16-slot array is derived with formulas (1)–(3) and also shown in Fig. 4. With the method, active resonant conductance distribution for the 32-slot array can also be derived.

In order to obtain the physical parameters of slots from the active resonant conductance distribution, the relationships between active resonant conductance and slot parameters are derived from 8 slots finite array model, as shown in Fig. 5 and Fig. 6. The corresponding relationships, obtained from a single slot model, are also shown in Fig. 5 and Fig. 6. It is worth noting that the discrepancy between active resonant conductance and self resonant conductance of slots increases greatly with offset. This means that mutual coupling in an SIW slot array is strongly dependent on slot offsets. Therefore, for high performance design requirement, mutual coupling in SIW slot array should be calculated carefully.

With these active resonant conductance relationships, the slot parameters including slot offset and length for 16-slot array are obtained from the calculated active resonant conductance distribution, as shown in Fig. 7(a). These relationships can also be used for the design of a large slot array with any number of slots; therefore, the physical parameters of the 32-slot array can also be derived, as shown in Fig. 7(b). It should be noted that the computational complexity does not increase as the number of slots in the designed array increases. This characteristic makes the proposed method suitable for the design of large slot arrays.

The 16-slot and 32-slot arrays designed by ARCM are simulated with HFSS software. The simulation results are shown in Fig. 8. The 20 dB return loss band of these arrays is from 22 GHz

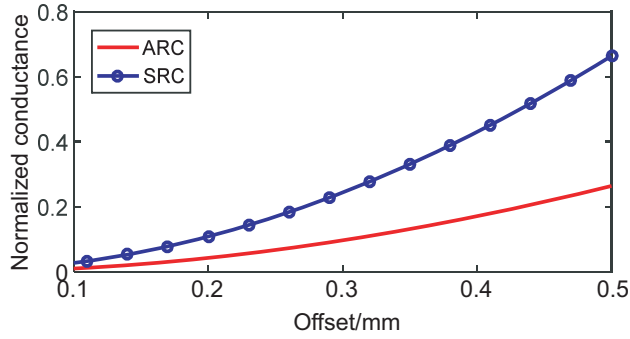


**Figure 5.** Active resonant conductance (ARC) and self resonant conductance (SRC) of slots.

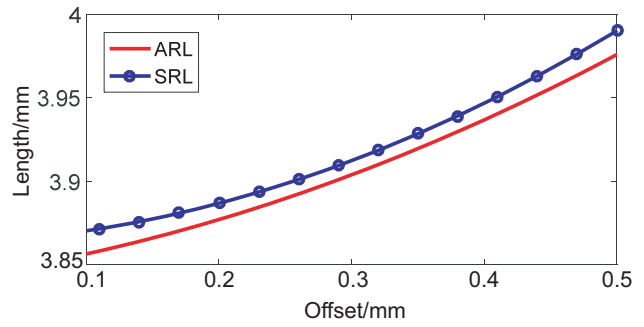


**Figure 6.** Active resonant length (ARL) and self resonant length (SRL) of slots.

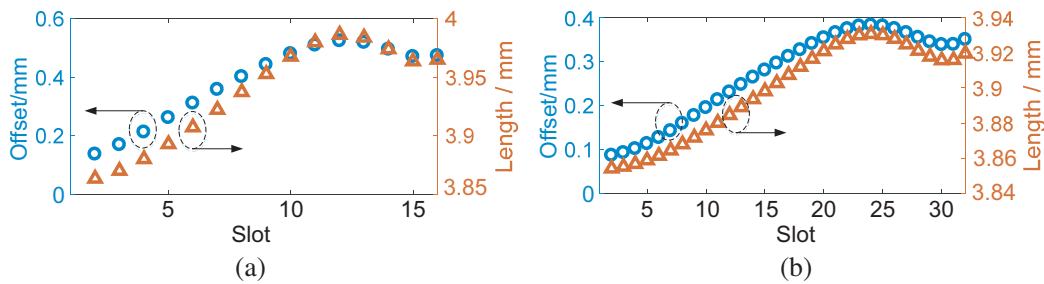


**Figure 7.** Offset and length of slots in the arrays. (a) The 16-slot array; (b) The 32-slot array.

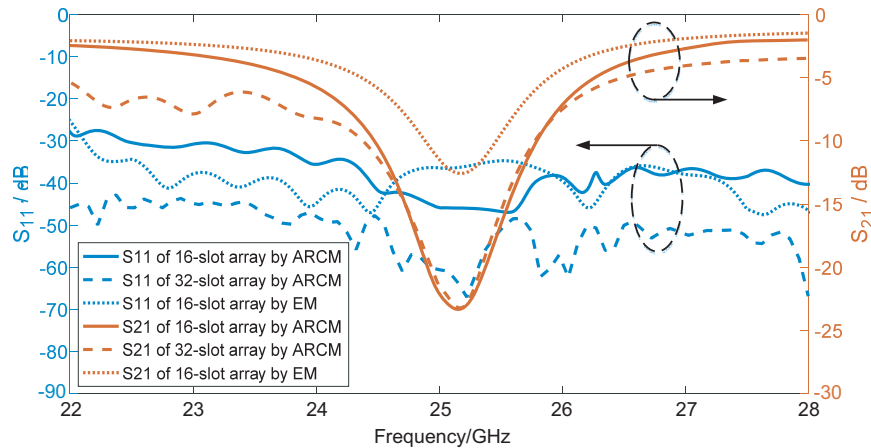


**Figure 8.** Simulated  $S$  parameters of the 16-slot and 32-slot arrays designed by the proposed ARCM and the 16-slot array designed by the Elliott’s method (EM).

to 28 GHz. The absorbed power of the matching load for these arrays ( $S_{21}$ ) is also shown in Fig. 8. At 25.16 GHz for 16-slot array and 25.17 GHz for 32-slot array, which are both very close to design center frequency  $f = 25.25$  GHz, the minimum power is absorbed by the matching load. In other words, the maximum power is radiated through the designed slot array. For comparison, the simulation results from the 16-slot array designed by the Elliott’s method (EM) are also shown in Fig. 8. The reflection coefficient from the 16-slot array designed by ARCM is very similar to that of the 16-slot array designed by EM. The power absorbed by the load in the 16-slot array designed by ARCM is lower than that from the 16-slot array designed by EM. It is caused by the calculation error of active resonant conductance for the peripheral slots.

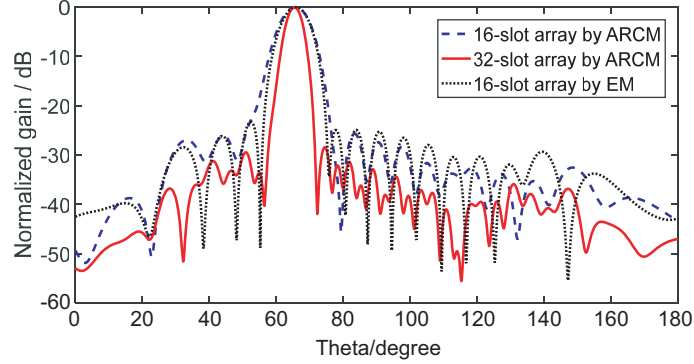


**Figure 9.** Simulated  $H$ -plane normalized pattern at 25.25 GHz for the 16-slot and 32-slot arrays designed by ARCM and the 16-slot array designed by EM.

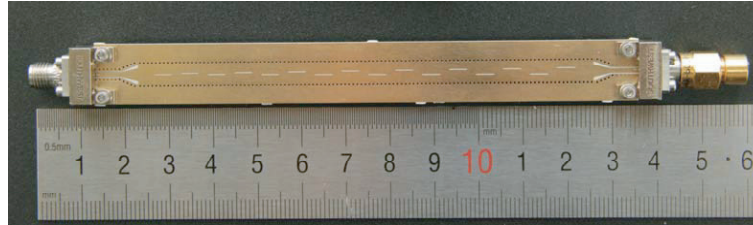


**Figure 10.** The traveling-wave-fed SIW slot array antenna with sixteen slots.

The simulated  $H$ -plane radiation patterns at center frequency  $f = 25.25$  GHz are shown in Fig. 9. The pattern from the 16-slot array designed by ARCM is very similar to that of the 16-slot array designed by EM, which verifies the accuracy of the proposed ARCM. The SLLs of the 16-slot array designed by ARCM are below  $-25.65$  dB, and that of the 32-slot array designed by ARCM is below  $-28.41$  dB. The SLLs obtained by the simulation and SLL design goals are in good agreement. The difference between simulated SLL and SLL design goal for the 16-slot and 32-slot arrays designed by ARCM is less than 2.6 dB. The difference is caused by calculation approximation of active resonant conductance for the peripheral slots. The gain of the 16-slot array designed by ARCM at center frequency  $f = 25.25$  GHz is 15.02 dBi, and that of the 32-slot array designed by ARCM is 17.10 dBi.

#### 4. FABRICATION AND MEASUREMENTS

The prototype of the 16-slot array designed by the proposed ARCM is fabricated, as shown in Fig. 10. Two symmetry tapered CPWG to SIW transitions are designed and aligned at the two ends of the slot array for feeding the array and connecting with load, respectively. Two same 2.92 mm female end launch connectors 1092-03A-6 from Southwest Microwave Corporation are soldered on the transitions for being compatible with the ports of measurement instruments and coaxial matching load. These CPWG to SIW transitions, demonstrated in Fig. 11(a), are optimized to match SIW and 50 Ohms CPWG over wide band [18]. The optimized parameters are  $W_0 = 1.18$  mm,  $S_0 = 0.15$  mm,  $W_t = 3$  mm,  $S_t = 0.65$  mm,  $L_t = 3.7$  mm. The measured  $S$  parameters of the back-to-back CPWG to SIW transition agree well with the trends of the simulated  $S$  parameters, as shown in Fig. 11(b). The difference in the magnitude is caused by coaxial connector loss and possibly slight misalignment in the measurement setup.

The return loss of the fabricated 16-slot array antenna is measured with Agilent vector network analyzer PNA E8363B. The simulated and measured return losses are shown in Fig. 12. Good agreement between measured return loss and simulated result for the 16-slot array with CPWG to SIW transitions is observed. The small discrepancy between measurement and simulation is caused by the simplified ideal coaxial connector models used in the simulation and imperfect fabrication dimensions. The measured

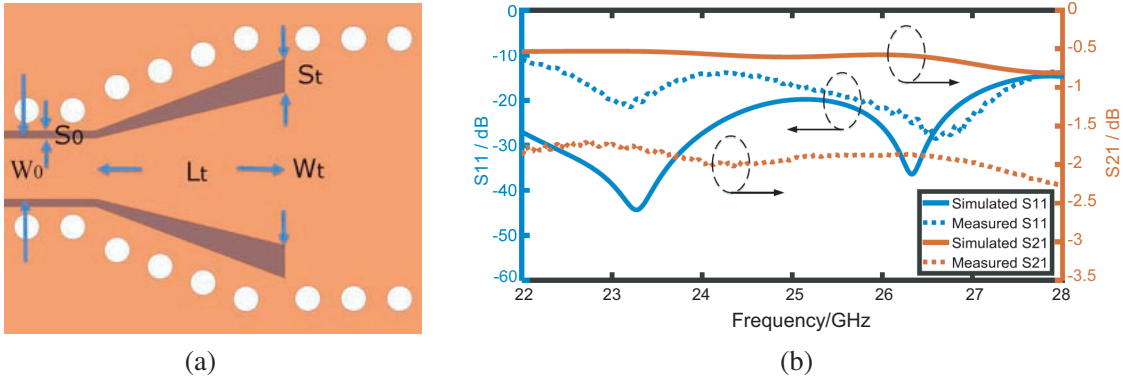


**Figure 11.** Tapered CPWG to SIW transition. (a) The sketch of the transition; (b) Simulated and measured  $S$  parameters of the back-to-back CPWG to SIW transition.

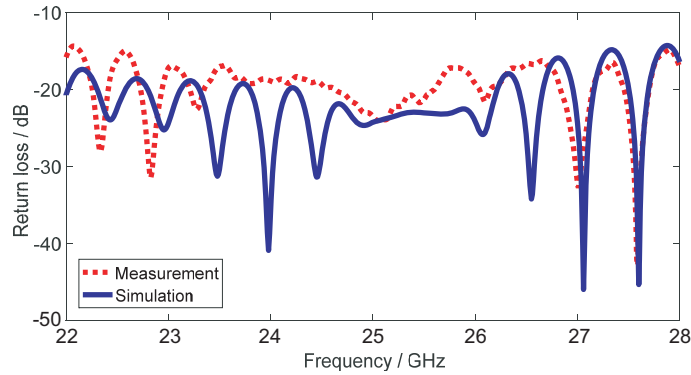


**Figure 12.** Measured and simulated return loss for the fabricated 16-slot array antenna.

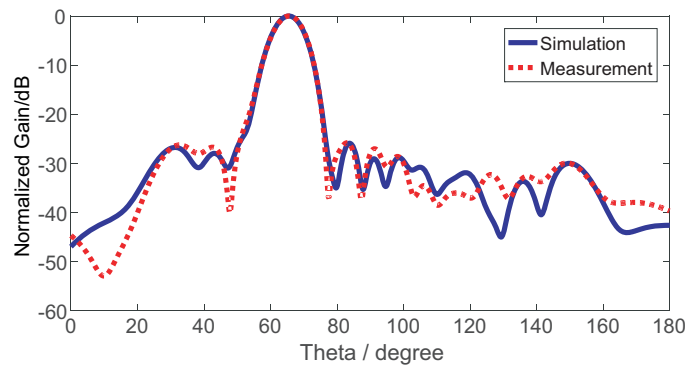


**Figure 13.** Measured and simulated  $H$ -plane pattern for the fabricated 16-slot array antenna.

15-dB return-loss band is from 22.14 to 27.87 GHz.

The  $H$ -plane radiation pattern of the fabricated 16-slot array antenna is measured in the compact antenna test range (CATR) of microwave engineering lab in Beihang University. In order to improve noise figure of the measurement system, a microwave system preamplifier 83051A (45 MHz–50 GHz) of Agilent is utilized. The simulated and measured  $H$ -plane radiation patterns at 25.25 GHz are shown in Fig. 13. The measured result which is in good agreement with the simulated result indicates that the SLLs in the  $H$ -plane are below  $-25.8$  dB, considerably low and close to the design goal. The simulated and measured gains also agree very well, and they are nearly constant around the center frequency, as

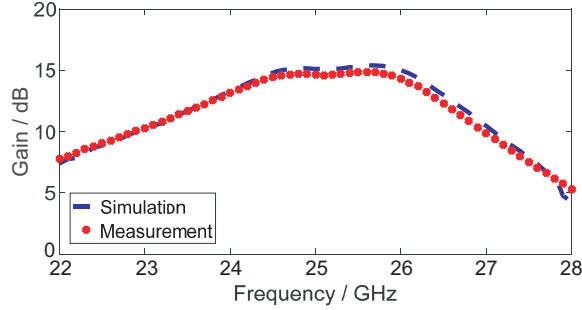


**Figure 14.** Simulated and measured gain for the fabricated 16-slot array antenna.

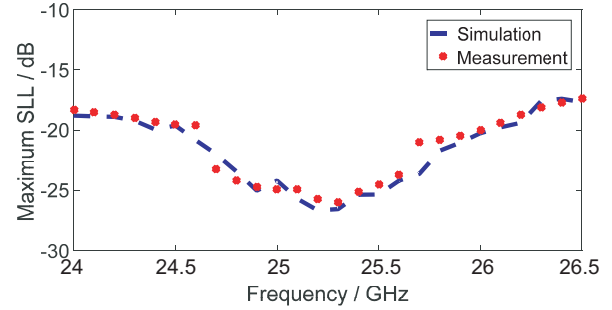


**Figure 15.** Simulated and measured maximum SLL for the fabricated 16-slot array antenna.

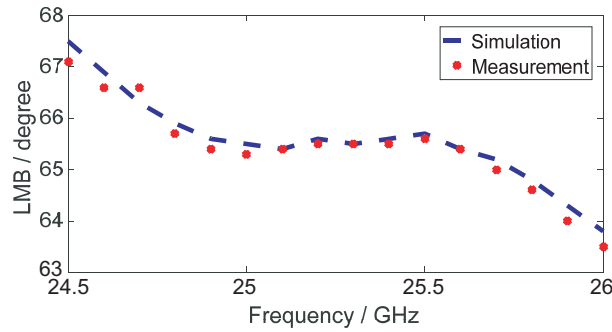


**Figure 16.** The location of main beam (LMB) in the simulated and measured radiation patterns.

shown in Fig. 14. The maximum gain is 15.40 dB in the simulation and 14.85 dB in the measurement. Considering the 3 dB criterion, the antenna measured gain bandwidth is 12.3% (23.5–26.6 GHz). The simulated and measured maximum SLLs are below  $-20$  dB from 24.5 GHz to 26 GHz, as shown in Fig. 15. The location of main beam is nearly constant from 24.75 GHz to 25.75 GHz, which is very similar to the result obtained in [10].

## 5. CONCLUSION

An active resonant conductance method for accurate design of large traveling-wave-fed SIW linear longitudinal slot arrays is presented. Two SIW slot arrays are designed and simulated, and one of them is fabricated and measured. Both simulated and measured results have verified the proposed method. In the method, both external and internal mutual couplings are considered with the intermediary active resonant conductance, which makes the proposed method very accurate and can be applied to low SLL application. The uniformly excited finite array model to calculate the active admittance of slots in array environment is independent of number of slots in a large designed array, which makes the proposed method feasible and efficient for the design of large traveling-wave-fed linear slot arrays. Simulation and measurement results show that the proposed method is suitable for design large traveling-wave-fed linear longitudinal slot arrays with good return loss and low sidelobe level.

## REFERENCES

1. Gilbert, R. A., “Waveguide slot antenna arrays,” *Antenna Engineering Handbook*, 4th Edition, Ch. 9, J. L. Volakis, Ed., McGraw-Hill, 2007.
2. Cassivi, Y., L. Perregrini, P. Arcioni, M. Bressan, K. Wu, and G. Conciauro, “Dispersion characteristics of substrate integrated rectangular waveguide,” *IEEE Microwave and Wireless Components Letters*, Vol. 12, No. 9, 333–335, 2002.

3. Deslandes, D. and K. Wu, "Accurate modeling, wave mechanisms, and design considerations of a substrate integrated waveguide," *IEEE Trans. Microwave Theory Tech.*, Vol. 54, No. 6, 2516–2526, 2006.
4. Feng, X. and K. Wu, "Guided-wave and leakage characteristics of substrate integrated waveguide," *IEEE Trans. Microwave Theory Tech.*, Vol. 53, No. 1, 66–73, 2005.
5. Yan, L., W. Hong, G. Hua, J. Chen, K. Wu, and T. J. Cui, "Simulation and experiment on SIW slot array antennas," *IEEE Microwave and Wireless Components Letters*, Vol. 14, No. 9, 446–448, 2004.
6. Liu, B., W. Hong, Z. Kuai, X. Yin, G. Luo, J. Chen, H. Tang, and K. Wu, "Substrate Integrated Waveguide (SIW) monopulse slot antenna array," *IEEE Trans. Antennas Propag.*, Vol. 57, No. 1, 275–279, 2009.
7. Xu, J. F., W. Hong, P. Chen, and K. Wu, "Design and implementation of low sidelobe substrate integrated waveguide longitudinal slot array antennas," *IET Microwaves, Antennas and Propagation*, Vol. 3, No. 5, 790–797, 2009.
8. Bakhtafrooz, A., A. Borji, B. Dan, and S. Safavinaeini, "Novel two-layer millimeter-wave slot array antennas based on substrate integrated waveguides," *Progress In Electromagnetics Research*, Vol. 109, 475–491, 2010.
9. Costanzo, S., G. A. Casula, A. Borgia, and G. Montisci, "Synthesis of slot arrays on integrated waveguides," *IEEE Antennas and Wireless Propagation Letters*, Vol. 9, 962–965, 2010.
10. Hosseininejad, S. E. and N. Komjani, "Optimum design of traveling-wave SIW slot array antennas," *IEEE Trans. Antennas Propag.*, Vol. 61, No. 4, 1971–1975, 2013.
11. Yang, H., et al., "Improved design of low sidelobe substrate integrated waveguide longitudinal slot array," *IEEE Antenna and Wireless Propagation Letters*, Vol. 13, 2014.
12. Yang, H., G. Montisci, Z. Jin, and Y. Liu, "Improved design of low sidelobe substrate integrated waveguide longitudinal slot array," *IEEE Antenna and Wireless Propagation Letters*, Vol. 14, 237–240, 2015.
13. Elliott, R. S. and L. Kurtz, "The design of small slot arrays," *IEEE Trans. Antennas Propag.*, Vol. 26, No. 2, 214–219, 1978.
14. Elliott, R. S., "On the design of traveling-wave-fed longitudinal shunt slot arrays," *IEEE Trans. Antennas Propag.*, Vol. 27, No. 5, 717–720, 1979.
15. Elliott, R. S., "An improved design procedure for small arrays of shunt slots," *IEEE Trans. Antennas Propag.*, Vol. 31, No. 1, 48–53, 1983.
16. Elliott, R. S. and W. O. Loughlin, "The design of slot arrays including internal mutual coupling," *IEEE Trans. Antennas Propag.*, Vol. 34, No. 9, 1149–1154, 1986.
17. Yee, H. Y., "The design of large waveguide arrays of shunt slots," *IEEE Trans. Antennas Propag.*, Vol. 40, No. 7, 775–781, 1992.
18. Yan, L., W. Hong, K. Wu, and T. J. Cui, "Investigations on the propagation characteristics of the substrate integrated waveguide based on the method of lines," *IEE Proceedings — Microwaves Antennas and Propagation*, Vol. 152, No. 1, 35–42, 2005.
19. Kazemi, R., A. E. Fathy, S. Yang, and R. A. Sadeghzadeh, "Development of an ultra wide band GCPW to SIW transition," *IEEE Radio and Wireless Symposium*, 171–174, 2012.